Non-Destructive Measurement Methods (Neutron-, X-ray Radiography, Vibration Diagnostics and Ultrasound) in the Inspection of Helicopter Rotor Blades

M. Balaskó[1], G. Endrőczi[2], Gy. Tarnai[3], I. Veres[4], Gy. Molnár[4], E. Sváb[5]

[1]KFKI Atomic Energy Res. Inst. H-1525 Budapest, POB. 49.
[2]Research Institute for Particles and Nuclear Physics; H-1525 Budapest, POB. 49
[3]Association of Hungarian Non-Destructive Inspectors for Material
[4]Aircraft Maintenance Branch of Hungarian Defense Force H-1525 Budapest, POB. 25
[5]Res. Inst for Solid State Physics and Optics H-1525 Budapest, POB. 49

ABSTRACT

The experiments regarding structural failures in helicopter rotor blade's composite structures causing water penetrations and bypasses were performed at the Dynamic Radiography Station (DRS) of the Budapest. As well as the structural integrity of repaired region were studied by applying dynamic neutron, X- ray radiographies and vibration diagnostics disclosed were horizontal and vertical primary and secondary percolation by-passes, the pore distribution patterns filled with water. The micro localization of structural failures were revealed and underlined by vibration diagnostics, too. Later our customers modified their requirements. Basically they wanted to avoid the risk of the human life by radiography techniques and instead of them, the semi-contactless vibration diagnostics and the ultrasound test were suggested. Thus a new measurement technology and strategy was developed. Ten pieces of reference sample were produced. First half of them did not contain any errors and the second half has contained one error per piece only. The results of the new methods were compared to the radiography pictures.

Keywords: *Neutron radiography, X-ray radiography, vibration diagnostics, semi-contactless vibration diagnostics, ultrasound test, helicopter rotor blades.*

1.0 INTRODUCTION

The affirmation of a structural failure in the rotary wing aircrafts, especially those of the rotor blades that can develop to a stage where structural integrity is affected comprises a central importance in the safe life testing. In this process the composition assessment, checking the rate growth of the defects in respect to the total flight hours are critical. As stated or mentioned above demands emphasize the necessity to test and apply non-destructive testing (NDT) methods for inspection in service [1]. According, to investigate the composite structure of the rotor blades, four NDT methods: (i) Neutron Radiography (NR), (ii) X-ray Radiography (XR), (iii) Vibration Diagnostics (VD) with Statistical Energy Analysis (SEA) and Ultrasound Test. (UT) were concurrently applied. These methods collect accessory information on the objects under inspection. The NR reveals deviations in the fiber-glass/epoxy honeycomb composition. The details of metal parts and are shown by XR.

The SEA and other VD methods are capable for localizing small alterations in structural damping, the UT gives information about the cracking of the spa of the rotor blade and about the bound between the spa and the sector.

Balaskó, M.; Endrőczi, G.; Tarnai, Gy.; Veres, I.; Molnár, Gy.; Sváb, E. (2005) Non-Destructive Measurement Methods (Neutron-, X-ray Radiography, Vibration Diagnostics and Ultrasound) in the Inspection of Helicopter Rotor Blades. In *Recent Developments in Non-Intrusive Measurement Technology for Military Application on Model- and Full-Scale Vehicles* (pp. 30-1 – 30-18). Meeting Proceedings RTO-MP-AVT-124, Paper 30. Neuilly-sur-Seine, France: RTO. Available from: http://www.rto.nato.int/abstracts.asp.

Report Documentation Page

Form Approved
OMB No. 0704-0188

1. REPORT DATE	2. REPORT TYPE	3. DATES COVERED
01 APR 2005	**N/A**	**-**

4. TITLE AND SUBTITLE	
Non-Destructive Measurement Methods (Neutron-, X-ray Radiography, Vibration Diagnostics and Ultrasound) in the Inspection of Helicopter Rotor Blades	5a. CONTRACT NUMBER
	5b. GRANT NUMBER
	5c. PROGRAM ELEMENT NUMBER
6. AUTHOR(S)	5d. PROJECT NUMBER
	5e. TASK NUMBER
	5f. WORK UNIT NUMBER
7. PERFORMING ORGANIZATION NAME(S) AND ADDRESS(ES) **KFKI Atomic Energy Res. Inst. H-1525 Budapest, POB. 49**	8. PERFORMING ORGANIZATION REPORT NUMBER
9. SPONSORING/MONITORING AGENCY NAME(S) AND ADDRESS(ES)	10. SPONSOR/MONITOR'S ACRONYM(S)
	11. SPONSOR/MONITOR'S REPORT NUMBER(S)

12. DISTRIBUTION/AVAILABILITY STATEMENT
Approved for public release, distribution unlimited

13. SUPPLEMENTARY NOTES
See also ADM202216., The original document contains color images.

14. ABSTRACT

15. SUBJECT TERMS

16. SECURITY CLASSIFICATION OF:			17. LIMITATION OF ABSTRACT	18. NUMBER OF PAGES	19a. NAME OF RESPONSIBLE PERSON
a. REPORT	b. ABSTRACT	c. THIS PAGE			
unclassified	**unclassified**	**unclassified**	**UU**	**18**	

According to the new requirement of the customer semi-contactless VD and ultrasound extended the measurement technology.

2.0 EXPERIMENTAL FACILITY

The experiments were performed at the Dynamic Radiography Station (DRS) of the Budapest reactor [2] where the necessary developmental work, with respect to the sizes of the rotor blades, was carried out. As a result, the reconstructed DRS can inspect 10 m long and 0.7 m wide targets (its weight is ~140 kg) by NR, XR and VD. The arrangement of the experimental set up is shown in Fig. 1.

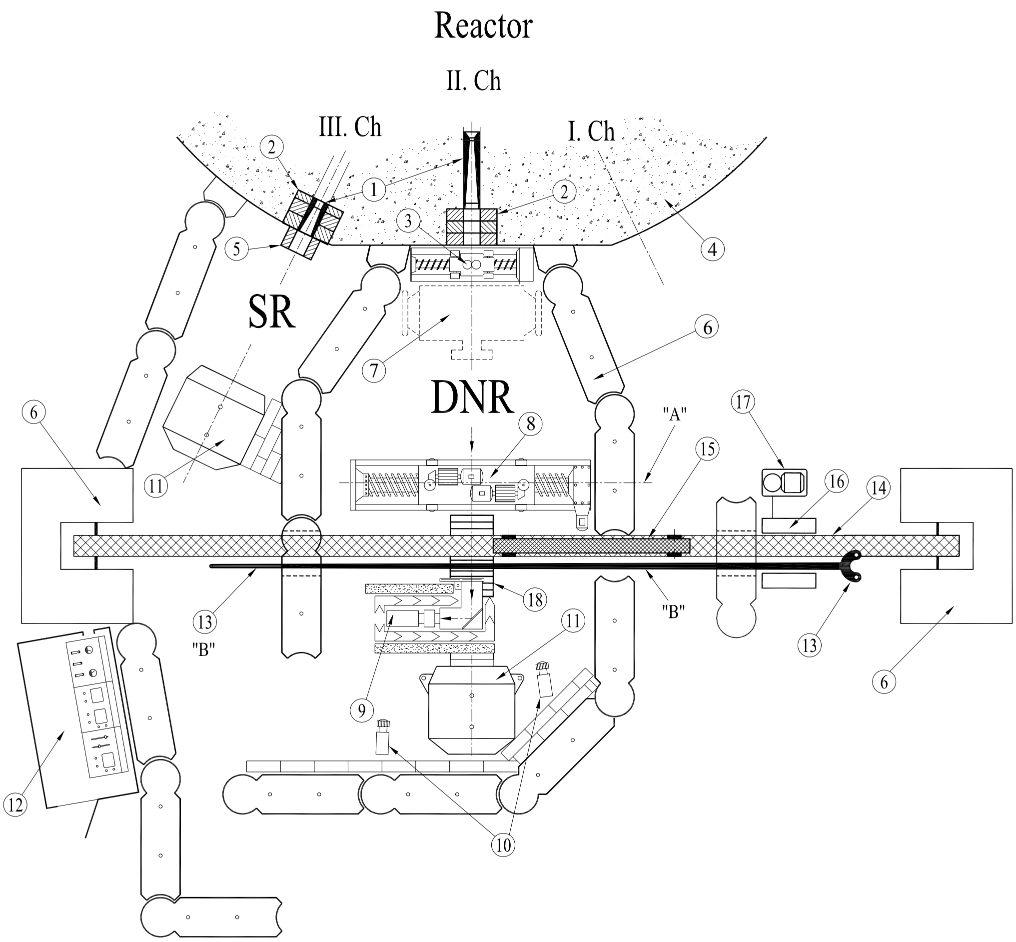

1. Inside collimator
2. Iron shutter system
3. Beam diameter changer and filter unit
4. Reactor shielding
5. Outside collimator
6. Biological shielding
7. X-ray generator
8. Investigated object with remote control mechanism
9. Imaging system with low light level TV camera
10. Background TV cameras
11. Beam stop
12. Control cabin
13. Rotor blade (~ 10 m)
14. Rail of the rotor blade transporter
15. Transporter of the rotor blade
16. Moistening module
17. High pressure water pump
18. Transporter rail of the Imaging system

Figure 1: Arrangement of the experimental set up of DRS.

The main parameters of the DRS are as follows: 10^8 $n \cdot cm^{-2} \cdot sec^{-1}$, the collimation ratio (L/D): 190, the diameter of the beam: 220 mm. The X-ray generator during the measurements had 150 kV voltages and 3 mA current. The obtained radiography images were converted into light one $ZnSAg/Li^6$ scintillator screen for neutron radiography and ZnS scintillator screen was used for X-ray radiography. The light images were sensed by a 10-bit CCD Photo Science camera (made in UK), cooled by double Peltier module. The camera offers a ~ 100 μm resolution. Imager-Pro Lite Version 3., and IMAN 2β version softwares were applied for digitalization and image processing, respectively.

The VD measurements were performed before and after the radiography tests. The arrangement of the VD measurement is shown in Fig. 2. The vibration sensors were placed at given points of the same sectors of blades, where NR and XR were accomplished, and the damping characteristics were collaterally studied with the radiography gauging. In addition to the Statistical Energy Analysis (SEA) measurement a small exciter table (BK4810) and impedance head (BK 8000) were used. The registered vibration noises were analyzed with a dual-channel real time frequency analyzer (BK2035).

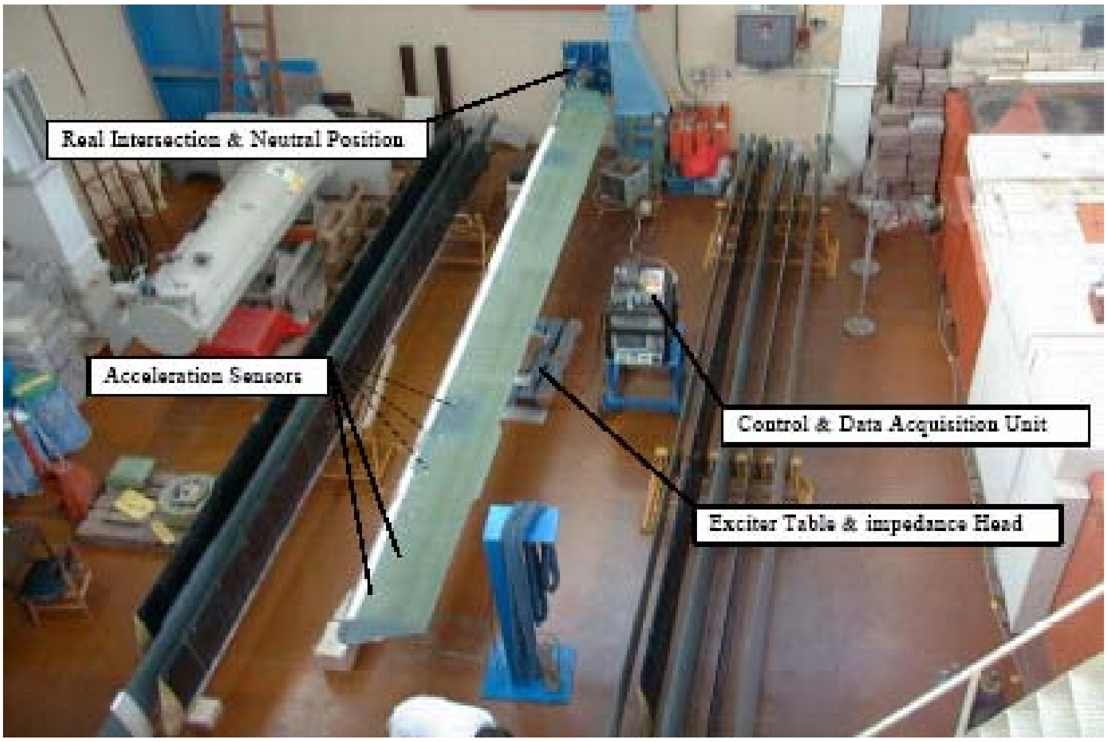

Figure 2: Arrangement of VD measurement in the Reactor Hall.

3.0 INVESTIGATED OBJECTS

Majority of the helicopters, Mi-8, Mi-17 and Mi-24 types in the Hungarian Army's inventory are several decades old and required to continue their service even longer. One of the most important parts of them is the rotor blade. They are made of composite structures and contain 21 pieces of honeycomb construction (sector) with many bonded surfaces. The 21 sectors of the rotor blades were divided into 4 bands horizontally and 53 columns in vertically [3], as it is shown in Fig.3. The key part of the rotor blade comprises the aluminum alloy metal main holder (spar) bonded to the honeycomb structure. „A" band gives information mainly about the state of trailing edge and the backside stringer. „B" band shows the state of the honeycomb structure.

State of the bonded area on the aluminum-alloy spar is represented by „C" band. The „D" band shows the state of the anti-ice heater and front edge of the rotor blade. Every exposed picture is characterized by a capital letter for the signal of the band and two numbers for selection of the field columns to identify its position on the rotor blades.

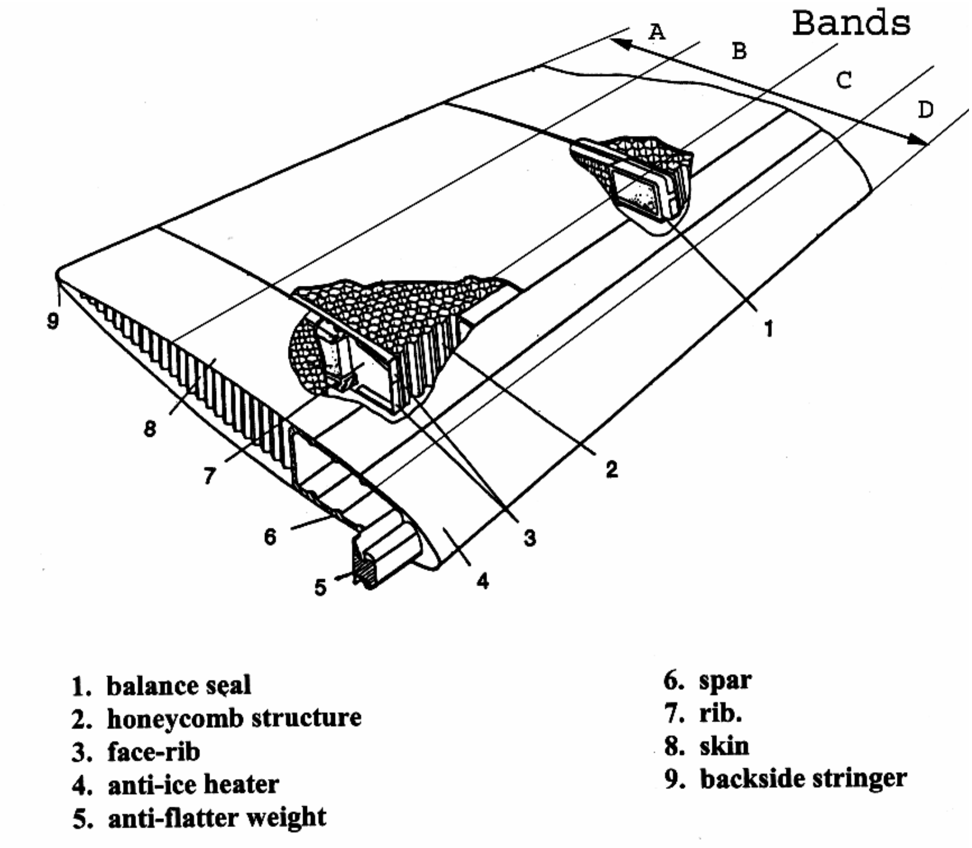

Figure 3: The inner structure of the rotor blade.

These identifiers were used as markers during the measurement. The markers (Cd) were positioned on the right-upper side corner of every exposed picture. It make easier to follow the extension of the errors between the different parts of the rotor blades. The territory of the exposed picture is 146x140 mm^2.

4.0 MEASUREMENT TECHNOLOGY

The description of the measurement was very prudent regarding the dangerous nature of the radiation material testing both neutrons and X-ray. On schedule of the inspection the first step was the vibration diagnostics (VD) measurement, the second step was an NR inspection in dry condition, the third step was the NR inspection in wet condition, the fourth step was the XR test and the last one another VD measurement again. Twenty-eight rotor blades were verified by this inspection technology in the last three years. We are able to declare that we did not experience any harmful effect of the radiation techniques.

4.1 Radiography Measurement

The measurement dealt to demonstrate the applicability of NR, XR and VD in revealing the defects of the composite structure of helicopter rotor blades. The radiography measurements were accomplished in three steps. In the first one, the all surface of the blade was scanned with NR in dry conditions. In the second one, having the rotor blade being moistened, the scanning operation was repeated to follow the penetration sites and distribution of water in the composite structures after the moistening procedure. In the third one the all surface of the rotor blade is scanned by XR. Regarding the large dimensions (its long is almost 10 m) of the rotor blades we had to divide into two parts of the investigated surface. The first one contains of the exposure fields from the end of the blade to the symmetry axis. After it is necessary to turn on the other side of the blades. In the second part of the scanning procedure we study from the driver end of the blade to the symmetry axis. 4 X 53 exposed pictures were collected in every radiography inspection step. The whole helicopter rotor blade was characterized by 612 exposed pictures after the radiography measurements. Two methods were applied to compose the whole radiography pictures of the helicopter rotor blades. The first one is available to give an approximate fast version of them (Approximate method) and the second one was developed for the precise well determinate composition (Rotor Puzzle method) of the whole rotor blade surface [3].

4.2 Vibration Diagnostics Measurement

The VD measurements were performed before and after the radiography tests. The vibration sensors were placed along the blade so to pick-up statistical information on sectors.

The phenomena of the energy exchange are shown in the Fig.4. Where K is a constant and (a) is the spatial average of acceleration. For SEA measurements a small exciter table (BK4810) via an impedance head (BK800) served for the energy input. The registered vibration responses were analyzed with a multi-channel real-time frequency analyzer (BK2035).

During the VD tests the blades were excited at the middlemost sector at the border of the metal main holder (spa) and the honeycomb structure and resulted vibration levels were picked-up with accelerometers placed at the sectors. The sweep-sine excitation covers the 1000Hz-9000Hz ranges. The level and other parameters of the vibration were calculated in 1kHz ranges from the measured spectrums.

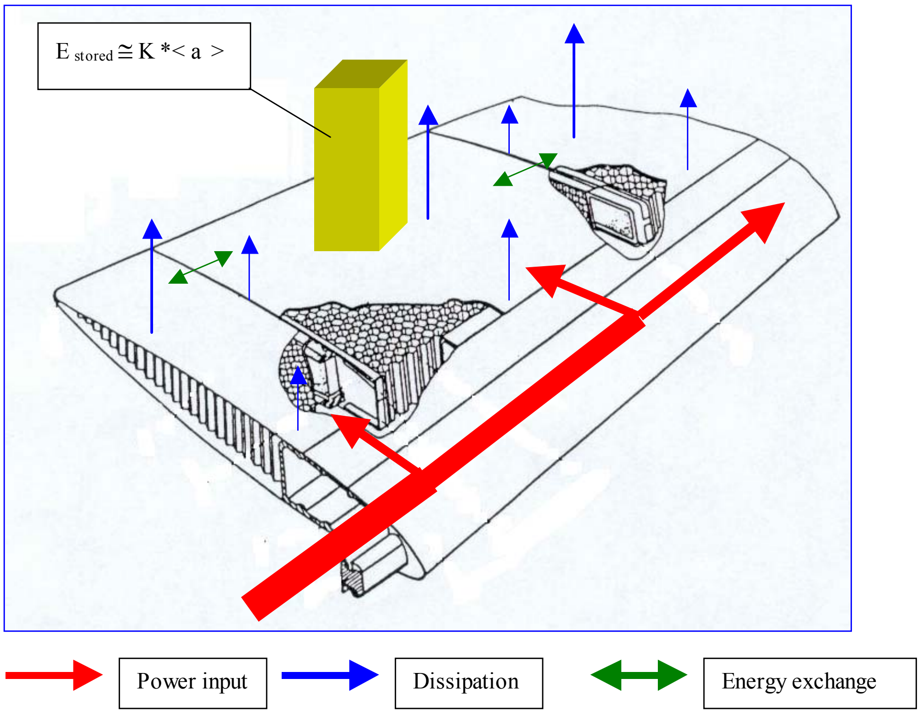

Figure 4: Energy exchange in the rotor blade.

4.3 Reference Objects

Later our customers modified their requirements. Basically they wanted to avoid the risk of the human life by radiography techniques and instead of them, the semi-contactless VD and the UT were suggested. A new measurement technology was developed by us. Ten pieces of reference sample were produced. First half of them did not contain any errors and the second half has contained one error per piece only. Never used spare sectors were applied as reference objects. The generated errors were the followings: demade of the honeycomb system, foreign material (inclusion) in the sector as it is shown in the Fig. 5., few resin in the honeycomb system, many resin in the honeycomb system and some drops water in the honeycomb system. Additional we have to produce some special sample for the UT. One of these is visible in the Fig.6., where it is lying in front of the original sector, which has a balance sheet. The results of the new methods were compared to the radiography pictures. A special adaptor was designed and made for moving of the reference objects as it is visible in the Fig. 7. The reference object has nine pieces markers for the identification of the exposed pictures. Behind of the original sector the aluminum holder of the scintillator screen and the light shielding tube of the CCD camera is observable. In front of the object, downstairs the passive brake system is visible, which reduced the vibration of the sector during the moving.

Figure 5: Metal inclusion (at the yellow arrow) in the reference object (original sector).

Figure 6: A lying special sample for ultrasonic test.

Figure 7: Reference object (original sector) in the exposure position.

4.4 Semi-Contactless Vibration Diagnostics Measurements

After due consideration a combination of contactless acoustical excitation and single detector has been tested last year. The main elements of the setup are shown on Fig. 8.

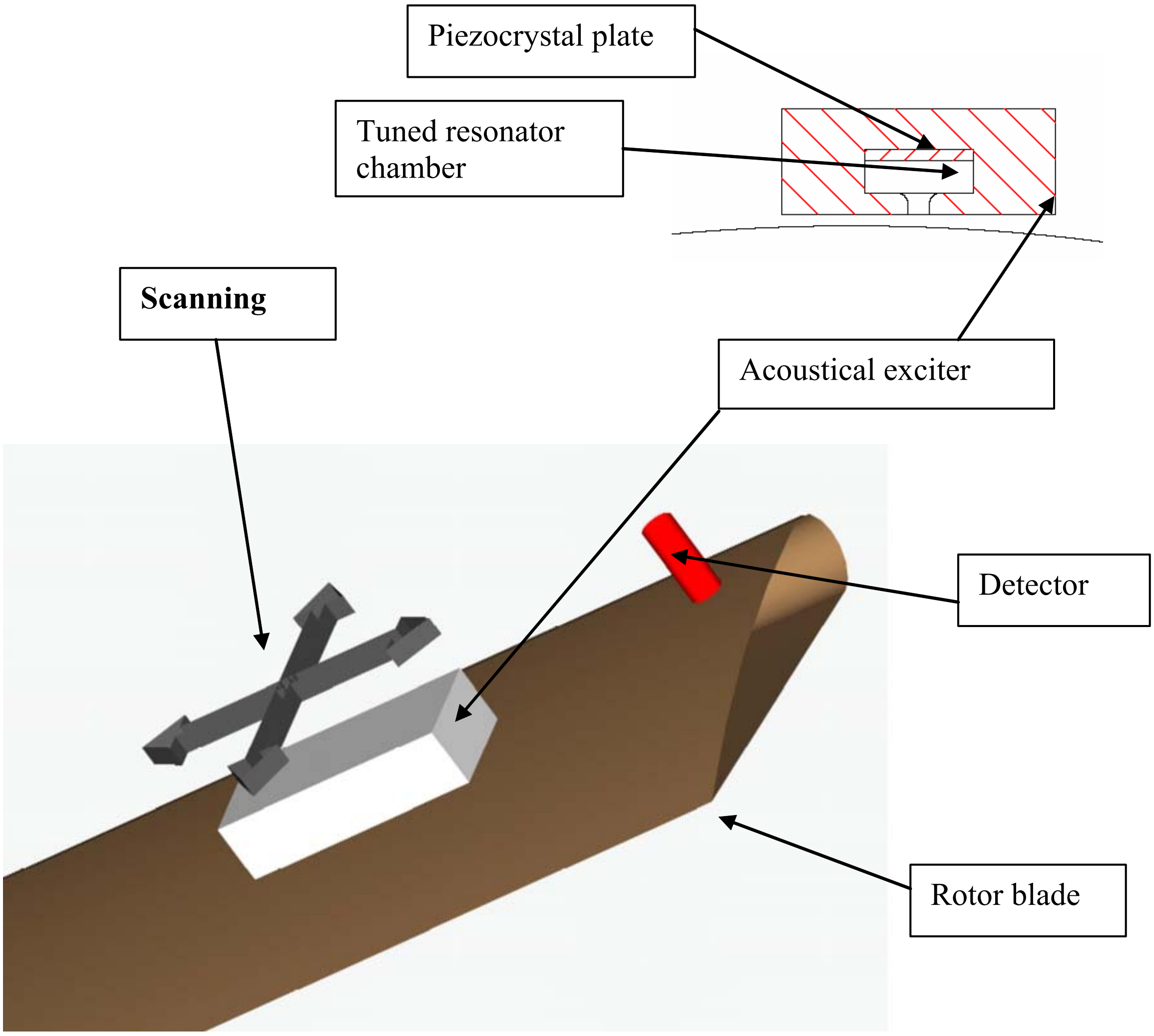

Figure 8: Experimental setup with contact less excitation.

The simple acoustical exciter based on "Helmholz resonator theory" gives a repeated impulse type mechanical excitation on the surface of blades. In our experiments the exciter was tuned so that the maximum power rose at 850Hz. The size of acoustical chamber and neck at this frequency produced enough power of "jets" to excite the blade within 2-3mm.

For the detection of response a high-frequency piezo-accelerometer was used.

4.5 Ultrasound Measurement

We had not any annotation to use UT for the inspection of helicopter rotor blade. An important decision was declared, that in the first time we deal only two categories of the errors. In the course of tests we have searched for the answers to the following questions:

- How can be applied the ultrasonic defectoscopy methods for inspection of the main spars' absence of cracks?
- Can be developed an ultrasonic method to the bond test of adhesive joints of main spar's to the cover-plat and to the sector?

In the tests, USM 35 type ultrasonic testing equipment and SMWB70-6 type probe were used.

On the outside and inside surface of main spar we placed crack like notches, of which direction are parallel with or perpendicular to the frame. The depth of notches was between 0.8-2 mm. To the configuration, because of practical thinking, we used etalons made of Fe, in that the ultrasonic wave velocity was different than in inspection piece, but this difference had no influence on the conceptual conclusion.

5.0 RESULTS

When we show the results of our experimental work in every measurements, the really events (error) will be shown by radiography techniques primary, after we try to follow the event (error) by VD on whole helicopter rotor blade, semi-contactless VD on reference object and UT on spatial object.

5.1 Result of the Vibration Diagnostics Measurement on Whole Helicopter Rotor Blades

Plenty of moisture was found inside the rotor blades. The moisture was characterized depending on its origin. The first category was where the water was identified in the dry state. The second one was where the water was found after the moistening procedure between the different sections. The third one was where the water was found after the moistening procedure inside of the sections behind of the fiber-glass/epoxy honeycomb structure. Fig. 9. shows the NR picture of the C27 picture field in dry (Fig. 9/a) and in wet (Fig. 9/b) state.

In consequence of various distortions, improper lay-up and porosity problems, connected with the flight hours or and other mechanical failures, reparation work on the honeycomb structure is needed in order to restore the integral stability of the blades.

In this respect to monitor the result of the reparation in service seems to be prerequisite. Fig. 10 shows the repaired area of the honeycomb structure of the B35 exposed picture field. It is clear that the reparation surface and its inner structure can only be investigated by NR (Fig. 10/a), while that of metal inclusion by XR in Fig. 10/b. The whole repaired area, as determined by NR imaging, was measured to be 27770 mm^2.

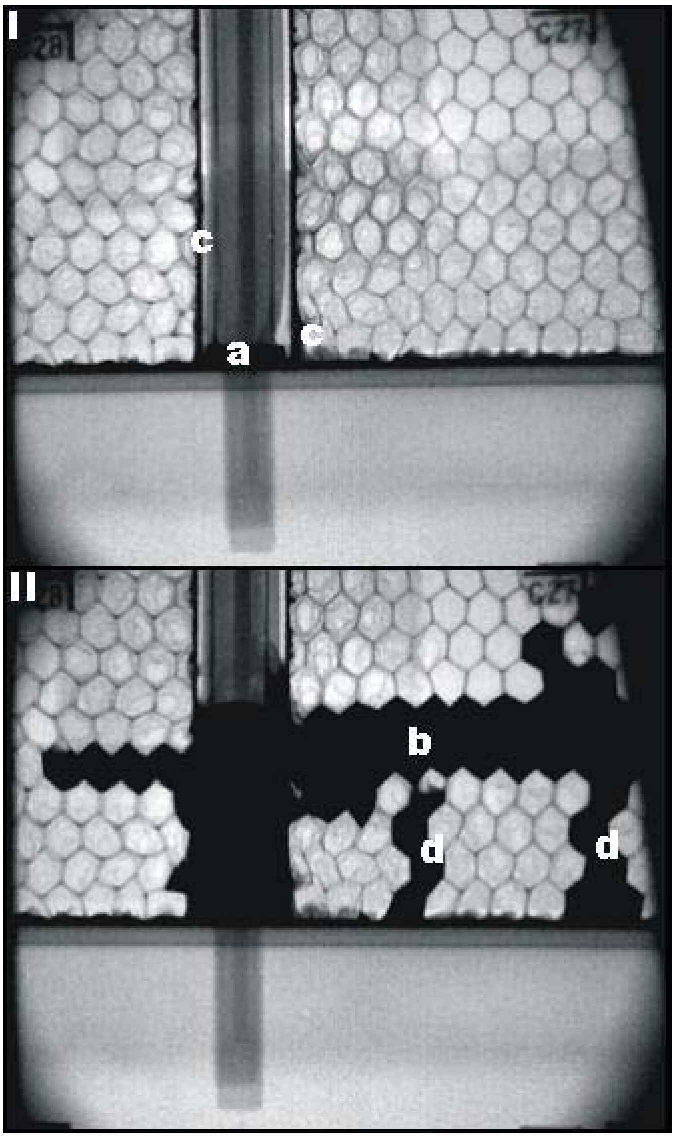

Figure 9/a: The NR picture of C27 exposed picture field in dry state (up).
Figure 9/b: The NR picture of C27 exposed picture field after the moistening procedure (down),
- a= support gum, b=horizontal by-pass, c= borders of the sector, d= vertical by-pass.

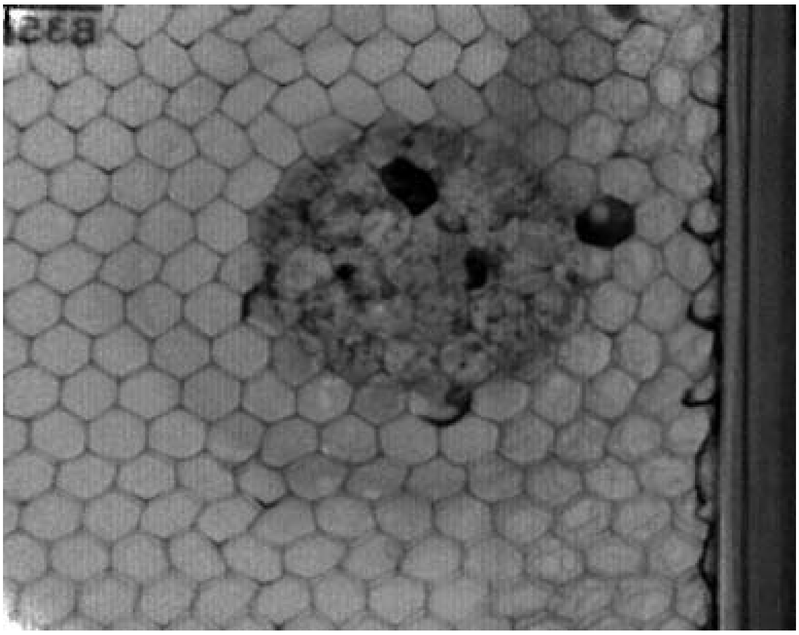

Figure 10/a: The NR picture B35 exposed picture field with the reparation area. The resin rich areas give darker contrast.

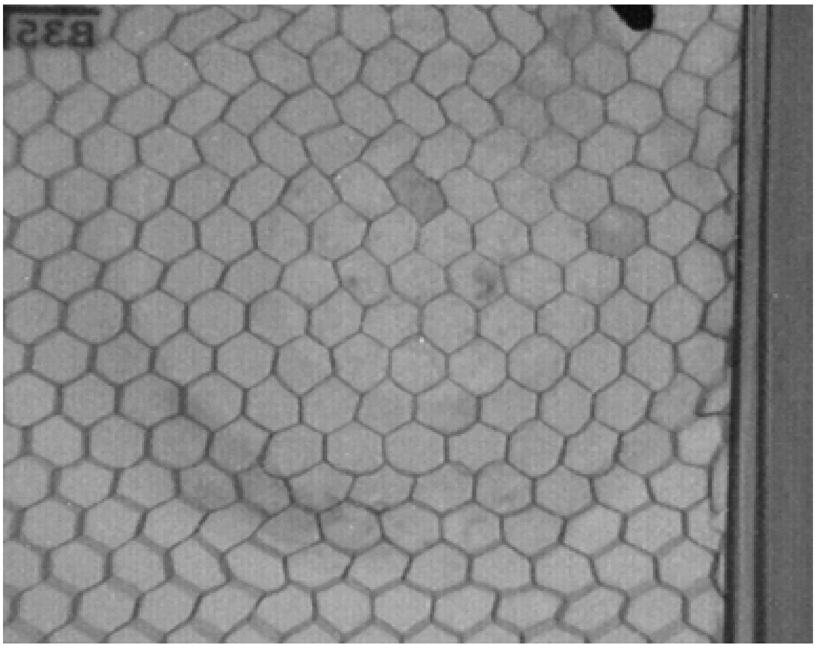

Figure10/b: XR picture B35 exposed picture field with the reparation area. The resin rich area hardly see but the metal inclusion is visible on the right-up corner.

The VD measurements were carried out before and after the radiographic tests. Thus the effect of penetrated water has been studied with this method too. During the VD tests the blades were excited at the middlemost sector at the border of the metal main holder and the honeycomb structure and resulted vibration levels were picked-up with accelerometers placed at the sectors. The sweep-sine excitation covers the 1000Hz-9000Hz ranges. The level and other parameters of the vibration were calculated in 1kHz ranges from the measured spectrums. The STD/AVR of frequency band is visible in Fig. 11

depending on the position of rotor blade. The STD is the standard deviation and the AVR is the average. The VD measurement is able to detect the rough errors in the rotor blade. Both the water percolation (C27) and place of the reparation (B35) are distinguishable.

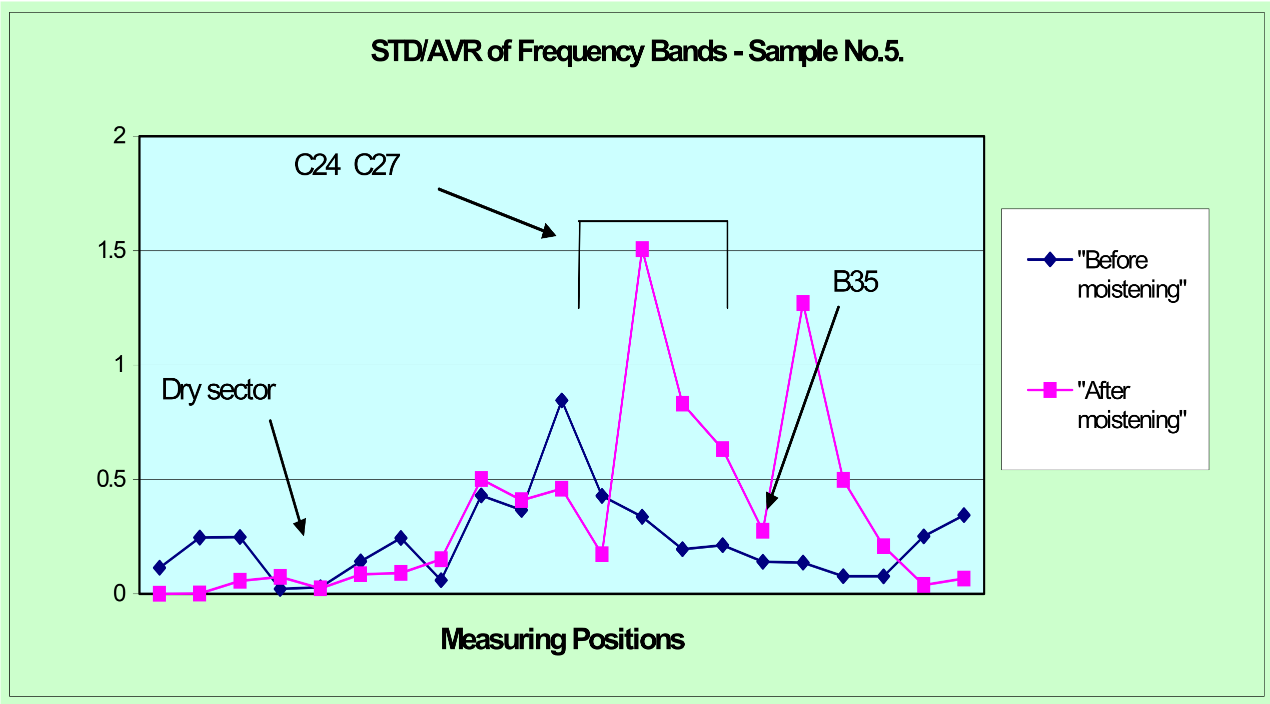

Figure 11: The STD/AVR of frequency band depending on the position of the rotor blade.

5.2 Results of the Semi-Contactless VD Measurements on Reference Object

A new measurement technology was developed by us to perform the modified requirements of the customer. Ten pieces of reference sample were produced. First half of them did not contain any errors and the second half has contained one error per piece only. Never used spare sectors were applied as reference objects. The Fig. 12 shows the NR picture of a metal inclusion in the Reference-2 object (see Fig. 5). The earlier experiments pointed out that the SEA theoretically suitable to detection of defects but the resolution of the method strongly depends on the applied excitation and measuring points. For detailed analysis of rotor blades the amount of required excitation and measuring points excludes the translation it into practical life.

The main goal of recent experiments is to find simple vibration methods with few detectors and excitation points for the detailed check. After due consideration a combination of contact less acoustical excitation and single detector has been tested last year. The main elements of the setup are shown in Fig. 8.

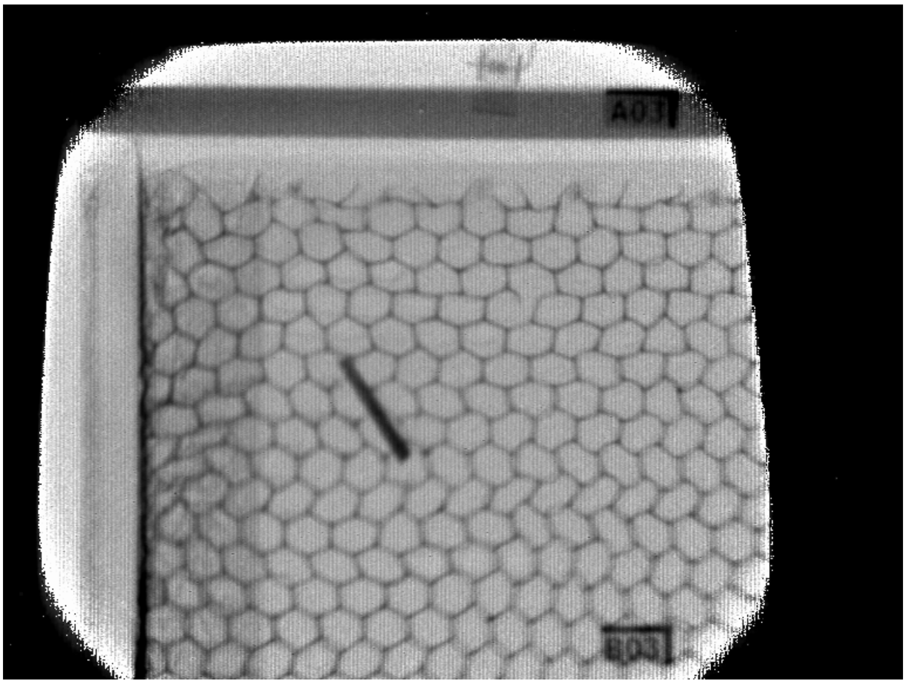

Figure12: NR picture of the A03 exposed picture field on the Reference-2 object with a metal inclusion in the middle of the field.

During the experiments of the defected Reference-2 object was scanned and analyzed in different frequency bands. Fig.13. shows the scanned vibration pattern of a defective blade part around 80kHz. The picture demonstrates that the small metal piece integrated in blade changes the local acoustical stiffness of the blade.

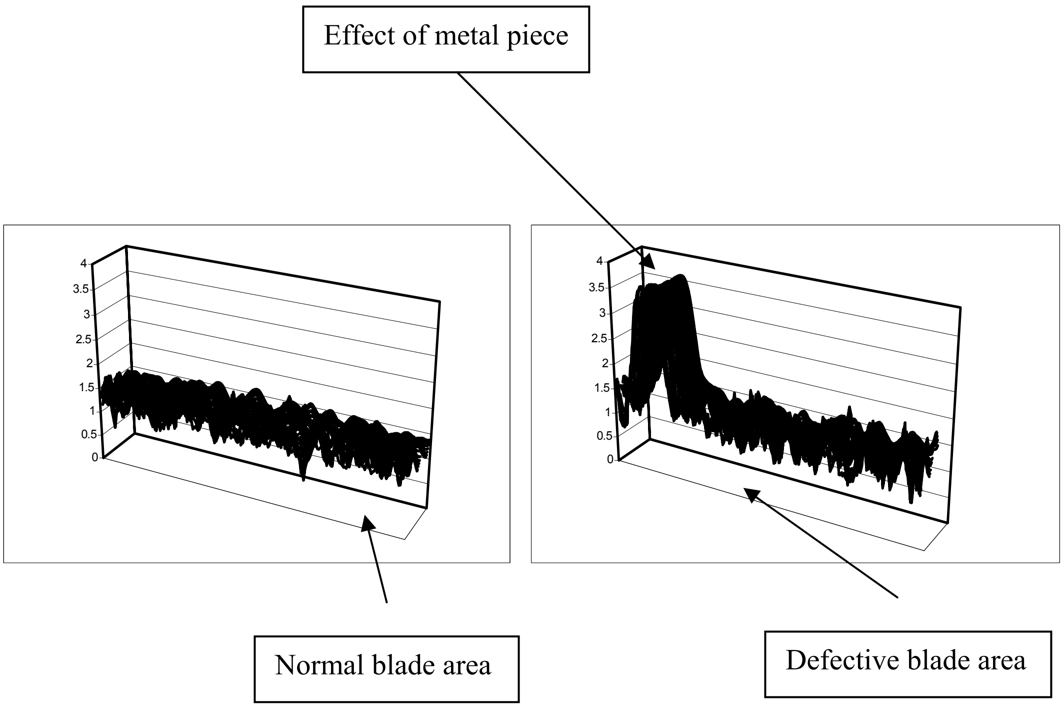

Figure13: Scanned acoustical pattern of metal piece defected blade.

Similar results appeared for deformed honeycomb structure and surface defects too.

The results of the first experiments indicate that the impulse like acoustical excitation might be a method for the detection of near surface defects.

5.3 Results of Ultrasound Test Measurements on Special Object

For the UT measurements a special object was produced (see Fig. 6.). Its XR picture (40 kV;2,5 mA) is shown in the Fig.14. It contains of some holes (diameter is 0,4mm) and some crack imitation (0,4 X 10 mm^2) in the material of aluminum alloy spa with the 6FE type wire picture quality indicator on the D44 exposed picture field. In the tests to detect the cracks of main spar's section we used the principle of ultrasonic physics that the significant part of energy, using the appropriate inspection technology, rebounds in echo form from the cracks. The test would be successful when the echoes descending from the cracks simulation in sections, clearly, are detected and can be located.

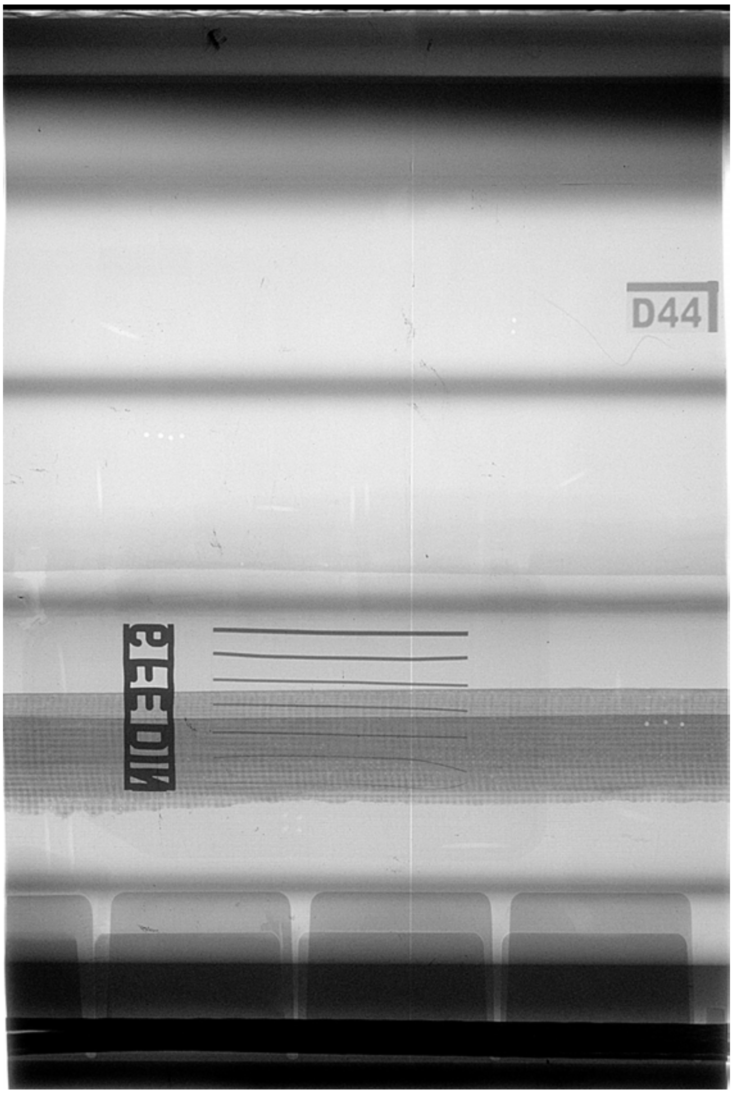

Figure 14: XR picture of the special object (D44 exposed picture field) for UT measurement contains of holes and imitation of cracks with 6FE type picture quality indicator.

In the course of tests we guided the inspection head all along on the outside surface of the main spar twice. In first case the direction of radiation was perpendicular to the frames, in second case it was parallel with frames. The equipment was calibrated to soundway-distance. The geometrical calibration of inspection unit (equipment, cable and probe), the measuring range was configured 0-100 mm. The inspection/testing amplification was 80 dB. In the case of detected „cracks" with probe approaching to notches from perpendicular direction, we grew the echo, which is proportional to the reflected ultrasonic energy, to the maximum. To recording A-picture, with the individual proportion, we decreased the volume of amplification. In the course of scanning all defects were detected successfully. In the following, we show A-pictures typical from point of view of inspection, through that the possibilities and limits of the method are interpreted well. On the Fig. 15 is shown A-picture of inspection, which is placed near the edge of main spar. On the figure three signals can be differentiated: main bang (left side), echo from the insection (middle)and the signal of energy rebounded (right side) from the edge of main spar (the first reflection rebounds from the crack [middle pick], the second from the edge of main spar [right pick]).

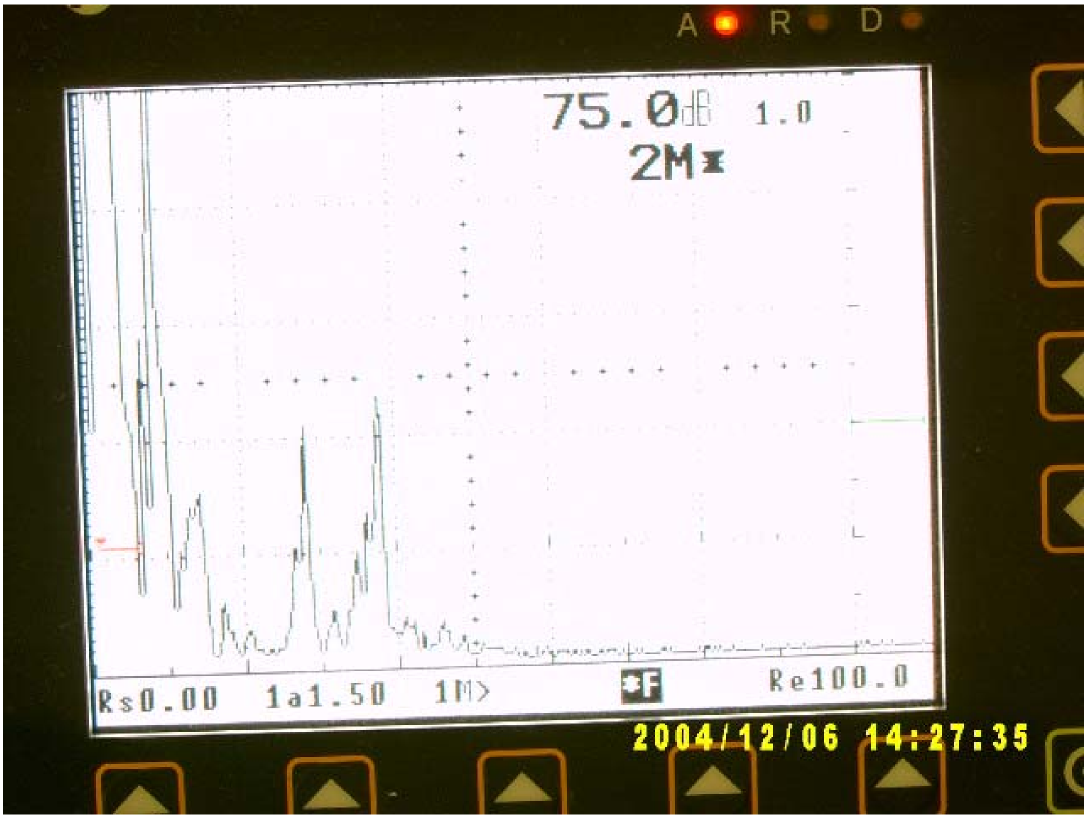

Figure 15: A-picture of insection, which is placed perpendicular to the frame, on the outside surface and near the edge of main spar.

Measuring range: 0-100 mm

Amplification: 75 dB

The ultrasonic tests developing method to inspection of bonded joint between section of main spar and cover-plate.

In the tests we used the principle of ultrasonic physics to the bond test of cover-plate that on the interface formed by the adhesive bonding the energy rebounding, or transition is related to the condition of bonding. In the measurements, USM 35 type ultrasonic testing equipment, DA312, K4N and DA301 type inspection probe were used. On the main spar, in some places, we cleaned the surface, in order to check the influential effects on the measure. On the main spars, at first, we recorded the backwall-echo, which received through the cleaned (from the cover) places and through the cover. After that, on two main spars, in same position, we performed ultrasonic inspection series in order to test the bonding of the cover-plate and main spar. In addition, we tried to „damage" the bonding condition with warming the main spar, and repeat the measures to demonstrate the changes of results of the ultrasonic tests.

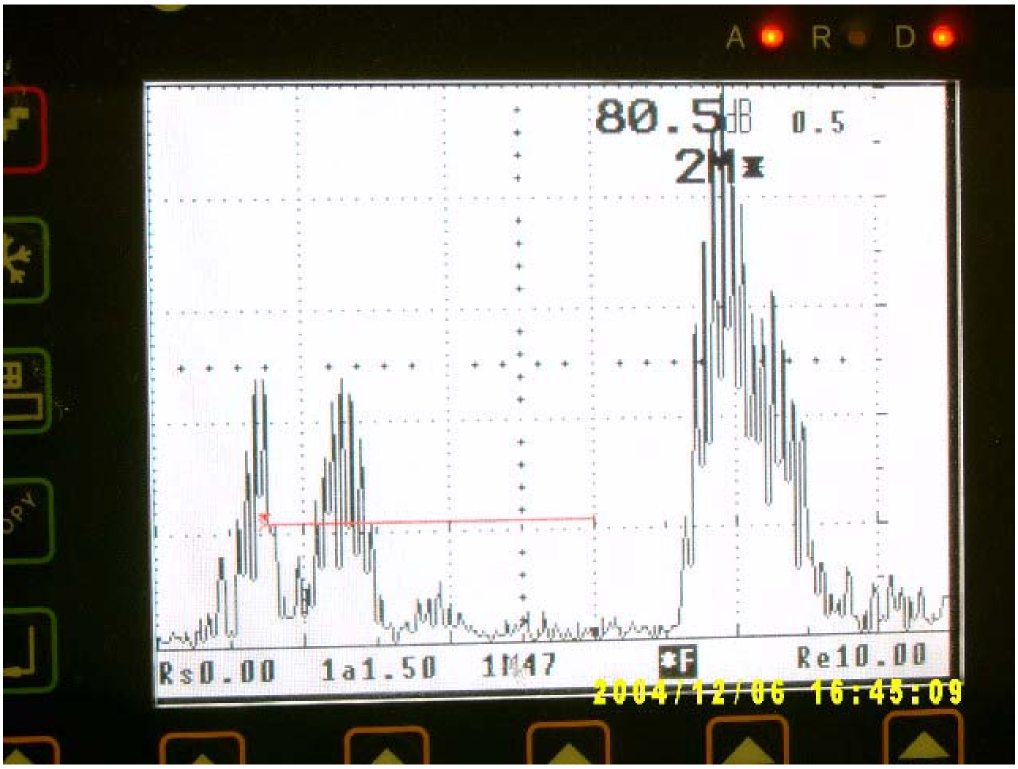

Figure 16: Bond test, Picture of A with application of inspection probe type DA 312.
Measuring range: 0-10 mm
Amplification: 80 dB

On the Fig. 16 this A-picture, which we received from ultrasonic test of an unknown quality joint. On this Figure two signal groups can be seen. The signal group A (left side) shows the range of the received reflection from surface of the joint view of cover-plate. The A signal group, practically, is approaching the echo scale that experienced by the measures of wall thickness. The B signal group (right side), means the radiant ultrasonic energy rebounding through the cover-plate, the adhesive bonding and the main spar.

6.0 CONCLUSION

Regarding the result of our experimental work we can declare the VD, the semi-contactless VD and the UT are available to detect the certain kinds of the errors, which were found by NR and XR techniques, as Inhomogeneous of the resin materials (resin-rich or starved areas) at the core-honeycomb surfaces; Defects at the adhesive filling; Water percolation at the sealing interfaces of the honeycomb sections; Quality control of resin-rich mended areas; Verification of the position of metal parts by X-ray; Corrosion effects study.

The advantage of the combined VD and SEA method the capability to inspect the whole helicopter rotor blade but the sensitivity and the resolution of it is limited compare to the semi-contactless VD. However the last one is able to detect the errors of the object with small dimensions only nowadays. The situation is similar to this with the UT method additional it is able to detect only the cracks and the de-bounds on the spa and the sectors recently.

REFERENCES

[1] M. Balaskó, G. Endrőczi, J. Veres, Gy. Molnár, F. Kőrösi, "Research of extension of the life cycle of helicopter rotor blade in Hungary." Proc NATO Conference for Applied Vehicle Technology Panel AVT-085 RSM-009, RTO Panel, Manchester, October 4-10, 2001, pp. 1-16.

[2] M. Balaskó, E. Sváb, Nucl. Instr. Meth. in Physics Res.. A377 (1996) 140.

[3] M. Balaskó, Zs. Balaskó, E. Balogh, A. Tanács, E. Katona, A. Kuba, Composition of radiography pictures of whole helicopter rotor blades in Hungary, Abstract book of 7th WCNR Rome, 15-20. September 2002, pp. 77-79.

[4] G.Endrőczi, Gy.Makai, J.Sári: Condition Monitoring of MI-8 Helicopter Rotor Blade with Statistical Energy Analysis; 7th Conf. on Vehicle System Dynamics, Identification and Anomalies (VSDIA2000), 6-8 Nov. 2000 Budapest, Proc. pp. 491-493.